

1 **Title: Pathogen-derived 9-methyl sphingoid base is perceived by a**
2 **lectin receptor kinase in *Arabidopsis***

3 **Authors:** H. Kato^{1*}, K. Nemoto², M. Shimizu², A. Abe², S. Asai³, N. Ishihama³, T.
4 Daimon¹, M. Ojika⁵, K. Kawakita⁵, K. Onai¹, K. Shirasu^{3,4}, M. Ishiura⁶, D. Takemoto⁵,
5 Y. Takano¹, R. Terauchi^{1,2*}.

6 **Affiliations:**

7 ¹Graduate School of Agriculture, Kyoto University, Kyoto, Japan.

8 ²Iwate Biotechnology Research Center, Kitakami, Japan.

9 ³RIKEN Center for Sustainable Resource Science, Yokohama, Japan.

10 ⁴Graduate School of Science, The University of Tokyo, Tokyo, Japan.

11 ⁵Graduate School of Bioagricultural Sciences, Nagoya University, Nagoya, Japan.

12 ⁶Graduate School of Science, Nagoya University, Nagoya, Japan.

14 *Corresponding authors: terauchi.ryohei.3z@kyoto-u.ac.jp (R.T.)

15 kato.hiroaki.6a@kyoto-u.ac.jp (H.K.)

17 **Abstract:**

18 In plants, many invading microbial pathogens are recognized by cell-surface pattern
19 recognition receptors (PRRs), inducing defense responses; yet how PRRs perceive
20 pathogen sphingolipids remains unclear. Here, we show that the ceramide Pi-Cer D
21 from a plant pathogenic oomycete *Phytophthora infestans* triggers defense responses
22 in *Arabidopsis*. Pi-Cer D is cleaved by an *Arabidopsis* apoplastic ceramidase, NCER2,
23 and the resulting 9-methyl-branched sphingoid base is recognized by a plasma
24 membrane lectin receptor-like kinase, RDA2. Importantly, 9-methyl-branched
25 sphingoid base, which is unique to microbes, induces plant immune responses by
26 interacting with RDA2. Loss of *RDA2* or *NCER2* function compromised *Arabidopsis*
27 resistance against an oomycete pathogen, indicating that these are crucial for defense.

1 We provide new insights that help elucidate the recognition mechanisms of pathogen-
2 derived lipid molecules in plants.

3

4 **One Sentence Summary:** Oomycete-derived ceramide is cleaved into sphingoid base
5 by ceramidase and recognized by an *Arabidopsis* receptor kinase.

6

7 **Main Text:**

8 Plant defend themselves against a multitude of microbial pathogens by sensing pathogen
9 invasion through cell-surface pattern recognition receptors (PRRs) that recognize
10 microbe- or pathogen-associated molecular patterns (MAMPs, PAMPs) or damage-
11 associated molecular patterns (DAMPs) of host-derived molecules that emanate from
12 damage caused by pathogen attack. This recognition then activates immune signaling (1-
13 3). The *Arabidopsis* genome contains genes encoding ~580 PRRs, including ~410
14 receptor-like kinases (RLKs) and ~170 receptor-like proteins (RLPs) that lack the kinase
15 domain (4). However, molecular interactions between MAMP/PAMPs and PRRs have
16 been demonstrated only in a limited number of cases, with the majority involving
17 pathogen peptides, proteins, and carbohydrates. It has recently been reported that lipids
18 derived from pathogens are also recognized by plant PRRs. The *Arabidopsis* PRR
19 LIPOOLIGOSACCHARIDE-SPECIFIC REDUCED ELICITATION recognizes
20 medium-chain 3-hydroxy fatty acids of bacterial pathogens (5), but whether other PRRs
21 recognize pathogen lipids remains unknown.

22 Ceramides belong to a class of sphingolipids consisting of a sphingoid base and
23 a fatty acid and are present at high concentrations in eukaryotic cell membranes.
24 Ceramide and its metabolites are also involved in intracellular signal transduction in
25 animal cells and plants (6-7). Recently, a ceramide-related compound, *Phytophthora*
26 *infestans* ceramide D (Pi-Cer D; Fig. 1A), from the oomycete pathogen *P. infestans* was
27 shown to induce immune responses in potato plants (8). Pi-Cer D also induced defense
28 responses in *Arabidopsis*; therefore, we aimed to identify the *Arabidopsis* components
29 involved in the perception of Pi-Cer D in *Arabidopsis*. For this, we employed Lumi-Map,
30 a platform consisting of a luciferase (LUC)-based mutant screen and gene identification
31 (fig. S1) (9). Because the *Arabidopsis* *WRKY33* gene is induced by PAMPs, including

1 flg22, a peptide derived from bacterial flagellin and is required for resistance against
2 pathogens (10-11), we tested whether Pi-Cer D induced the expression of a *LUC*
3 transgene driven by the *WRKY33* promoter (p*WRKY33-LUC*) in Arabidopsis, which
4 resulted in a transient induction of bioluminescence (fig. S2). We then screened 10,000
5 M₂ seedlings generated by ethylmethanesulfonate (EMS) mutagenesis of the p*WRKY33-*
6 *LUC* reporter line (W33-1B) for mutants that showed a reduction in bioluminescence
7 after Pi-Cer D treatment (named Low (L) mutants). We isolated nine mutants insensitive
8 to Pi-Cer D (L-09, L-12, L-16, L-19, L-31, L-46, L-55, L-66, and L-74) and two mutants
9 with an extremely low response to Pi-Cer D (L-53 and L-107) (Fig. 1B and fig. S3, Table
10 S1). These mutants showed normal bioluminescence responses to other PAMPs, such as
11 flg22, elf18, derived from bacterial elongation factor Tu, and chitin, a component of
12 fungal cell walls, indicating that they carried lesions affecting the signaling pathway that
13 is specifically required for the response to Pi-Cer D (Fig. 1C and fig. S4). To identify the
14 gene(s) altered in these mutants, we performed MutMap analysis (12). All nine Pi-Cer D-
15 insensitive mutants showed SNP-index peaks on chromosome 1 and contained SNPs
16 within the gene *At1g11330* encoding a lectin receptor-like kinase RDA2 (resistant to
17 DFPM-inhibition of ABA signaling 2) (Fig. 1D, fig. S5, and Table S2), a mutant of which
18 (*rda2*) is insensitive to a small synthetic molecule [5-(3,4-dichlorophenyl)furan-2-yl]-
19 piperidine-1-ylmethanethione (DFPM) and incapable to mount DFPM-mediated immune
20 signaling and inhibition of ABA signaling (13). Thus, we tentatively named the nine Pi-
21 Cer D-insensitive mutants as *rda2-4* through *rda2-10*. The two Pi-Cer D low-response
22 mutants showed SNP-index peaks on chromosome 2 and carried mutations in the gene
23 *At2g38010*, which encodes neutral ceramidase 2 (*NCER2*, Fig. 1E, fig. S5, and Table S2)
24 (14). We then tentatively named L-53 and L-107 mutants as *ncer2-2* and *ncer2-3*,
25 respectively. Complementation of the *rda2* and *ncer2* mutant lines by the respective wild-
26 type alleles restored bioluminescence induction following Pi-Cer D treatment, confirming
27 that *RDA2* and *NCER2* are the responsible genes for the given phenotypes (Fig. 1F and
28 fig. S6). Furthermore, T-DNA insertion mutant lines for *RDA2* and *NCER2* showed either
29 no or reduced induction of *WRKY33* gene expression after Pi-Cer D treatment (fig. S7).
30 Collectively, these results indicate that *RDA2* and *NCER2* are required for Pi-Cer D
31 recognition in Arabidopsis. We then asked whether *RDA2* and *NCER2* contribute to
32 Arabidopsis immunity against an oomycete pathogen *Hyaloperonospora arabidopsis*.
33 Importantly, both *rda2* and *ncer2* mutants showed increased susceptibility to *H.*

1 *arabidopsis* (Fig. 1G), indicating that *RDA2* and *NCER2* are required for resistance to
2 this pathogen.

3 We hypothesized that (i) Pi-Cer D is cleaved by NCER2 into a mature ligand product
4 in the apoplastic space and (ii) the ligand is recognized via plasma-membrane-localized
5 RDA2. To test the first hypothesis, we investigated whether the *ncer2* mutant phenotype
6 was rescued by the product generated by NCER2 ceramidase treatment of Pi-Cer D (Fig.
7 2A). The lipid fraction containing Pi-Cer D and NCER2 produced in *Nicotiana*
8 *benthamiana*, as well as that containing Pi-Cer D and a mouse ceramidase, induced
9 p*WRKY33-LUC* bioluminescence in the *ncer2-2* mutant (L-53) (Fig. 2B). We observed
10 no bioluminescence when we used NCER2^{G46S}, a mutant version of NCER2 present in
11 *ncer2-3* (L-107). These results indicate that Pi-Cer D was cleaved by NCER2-encoded
12 ceramidase and the resulting compound was recognized by RDA2. The predicted
13 molecular size of NCER2 tagged with hemagglutinin (HA-NCER2) was 82 kDa; however,
14 the protein detected by immunoblot analysis using anti-HA antibody was 26 kDa (fig.
15 S8). Upon purifying the HA-NCER2 protein and subjected it to gel electrophoresis, we
16 recovered two protein bands (26 kDa and 56 kDa) (fig. S8). Analysis of the bands by
17 liquid chromatography-tandem mass spectrometry (LC-MS/MS) revealed that they
18 corresponded to the N- and C-terminal regions of NCER2 (Table S3), respectively. These
19 results indicate that NCER2 is processed into its N- and C-terminal regions, which
20 function together. To investigate the localization of NCER2, we then generated transgenic
21 *Arabidopsis* *ncer2-2* mutant lines that expressed HA-NCER2 driven by its own promoter
22 (*ncer2-2 HA-NCER2*) (fig. S9). We detected the HA-NCER2 protein in the apoplast wash
23 fluid (AWF) of these lines (Fig. 2D) and found that *WRKY33-LUC* activity was induced
24 in the AWF from the wild-type reporter line and *ncer2-2 HA-NCER2* lines, but not in that
25 from the *ncer2-2* mutant (Fig. 2C). These results indicate that NCER2 localized to the
26 apoplast and metabolizes Pi-Cer D into a mature ligand product that is recognized by
27 RDA2.

28 Mass spectrometry analysis of compounds in the lipid fraction prepared from a
29 mixture of Pi-Cer D and ceramidase detected a sphingoid base, suggesting that the
30 sphingoid base derived from Pi-Cer D might be the ligand for RDA2 (fig. S10). We also
31 compared the *WRKY33-LUC*-inducing activity of Pi-Cer D analogs, which revealed that
32 structural differences in the sphingoid base determine the level of induction (fig. S11).
33 The sphingoid base in Pi-Cer D ((4E,8E,10E)-9-methyl-4,8,10-sphingatrienine,

1 9Me,4E,8E,10E-d19:3) contains a unique branching methyl group at the ninth carbon
2 position. Remarkably, this 9-methyl-branched structure is present in sphingoid bases of
3 oomycete, fungi and marine invertebrates, but has not been reported in plants and
4 mammals (15-17). We thus hypothesized that the 9-methyl-branched structure of the
5 sphingoid base is decisive in distinguishing between ‘self’ and ‘nonself’ in plants.
6 Therefore, we investigated the ability of various sphingoid bases to induce a defense
7 response. Because the sphingoid base in Pi-Cer D (9Me,4E,8E,10E-d19:3) was difficult
8 to obtain, we used (4E,8E)-9-methyl-4,8-sphingadienine (9Me,4E,8E-d19:2, hereafter
9 9Me-Spd) to evaluate 9-methyl structure (Fig. 3A). Notably, the *rda2* mutants were
10 almost insensitive to 9Me-Spd, indicating that 9Me-Spd is specifically recognized by
11 RDA2 (fig. S12). Among the sphingoid bases we tested, 9Me-Spd showed the strongest
12 RDA2-dependent elicitor activity (Fig. 3B, 3C, fig. S12 and S13). In addition, (4E,8E)-
13 4,8-sphingadienine (4E,8E-d18:2, Spd) and sphingosine (4E-d18:1, Sph), neither of
14 which contain 9-methyl branching, also showed elicitor activity, although this was
15 significantly weaker than that of 9Me-Spd (Fig. 3C, figs. S12 and S13). To identify the
16 structural correlates of RDA2-dependent sensing of the sphingoid base, we tested
17 sphingosine derivatives with different lengths of long-chain bases. Among these
18 derivatives, Sph (4E-d18:1) induced the highest bioluminescence in the pWRKY33-LUC
19 reporter line, followed by 4E-d16:1, 4E-d14:1, and 4E-d12:1 (fig. S14). This indicates
20 that efficient sensing by RDA2 requires a long-chain base structure that includes 18
21 carbon atoms. We also tested phytosphingosine (4-hydroxysphinganine, 4-t18:0, PHS)
22 and found that it did not elicit bioluminescence in the pWRKY33-LUC reporter line. This
23 indicates that the 4E double-bond structure in Sph is crucial for its sensing by RDA2 (fig.
24 S15).

25 To further investigate the downstream events following RDA2-mediated sensing, we
26 tested the ability of 9Me-Spd and its derivatives to activate *Arabidopsis* immune
27 responses. The 9Me-Spd activated RDA2-dependent bioluminescence induction,
28 transcript accumulation of defense-related genes (*FRK1*, *At1g51890*), phosphorylation of
29 mitogen-activated protein kinases, and the production of reactive oxygen species (ROS)
30 more strongly than Spd and Sph (Fig. 3C-F and fig. S12). A protein-lipid overlay assay
31 using a membrane fraction containing HA-tagged RDA2 demonstrated physical
32 interaction between 9Me-Spd and RDA2 (Fig. 3G, fig. S16 and S17). Collectively, these

1 results suggest that RDA2 is the receptor for sphingoid bases including 9-methyl
2 sphingoid base, which is derived from Pi-Cer D.

3 Sphingolipids are major components of eukaryote membranes (16-18). Our findings
4 revealed that oomycete-derived ceramide is cleaved by plant apoplastic ceramidase and
5 the generated sphingoid base is recognized by a lectin receptor-like kinase (Fig. 4). This
6 indicates that plants perceive differences in sphingolipid structure for non-self
7 recognition. Notably, plant RDA2 senses the 9-methyl-branching structure of sphingoid
8 bases that are prevalent in oomycetes and fungi. It has recently been reported that *RDA2*
9 is required for immune signaling and inhibition of ABA signaling by a small synthetic
10 molecule DFPM as identified by a chemical genetic screen (13). We hypothesize that
11 DFPM or its metabolized product functions as a mimic of sphingoid base, but further
12 study is required to clarify this. Based on our results, we propose the name *SphingR* (for
13 *sphingoid recognizing*) as a synonym of *RDA2* (Fig. 4). Our study here provides a basis
14 on which to engineer RDA2/SphingR to detect various pathogen-specific lipids and to
15 enable plants mount defense against pathogens such as *P. infestans*, the causal agent of
16 the potato late blight that devastated potato crop and caused famine in the nineteenth
17 century.

18

19 **References and Notes:**

20 1. F. Boutrot, C. Zipfel, Function, discovery, and exploitation of plant pattern recognition
21 receptors for broad-spectrum disease resistance. *Annu. Rev. Phytopathol.* **55**, 257-
22 286 (2017). [doi: 10.1146/annurev-phyto-080614-120106](https://doi.org/10.1146/annurev-phyto-080614-120106)

23

24 2. S. Ranf, Sensing of molecular patterns through cell surface immune receptors. *Curr.*
25 *Opin. Plant Biol.* **38**, 68-77 (2017). [doi: 10.1016/j.pbi.2017.04.011](https://doi.org/10.1016/j.pbi.2017.04.011)

26

27 3. D. H. Lee, H. S. Lee, Y. Belkhadir, Coding of plant immune signals by surface
28 receptors. *Curr. Opin. Plant Biol.* **62**, 102044 (2021). [doi:
29 10.1016/j.pbi.2021.102044](https://doi.org/10.1016/j.pbi.2021.102044)

30

31 4. D. Tang, G. Wang, J. M. Zhou, Receptor Kinases in Plant-Pathogen Interactions: More
32 Than Pattern Recognition. *Plant Cell.* **29**, 618-637 (2017). [doi: 10.1105/tpc.16.00891](https://doi.org/10.1105/tpc.16.00891)

1

2 5. A. Kutschera, C. Dawid, N. Gisch, C. Schmid, L. Raasch, T. Gerster, M. Schäffer, E.
3 Smakowska-Luzan, Y. Belkhadir, A. C. Vlot, C. E. Chandler, R. Schellenberger, D.
4 Schwudke, R. K. Ernst, S. Dorey, R. Hückelhoven, T. Hofmann, S. Ranf, Bacterial
5 medium-chain 3-hydroxy fatty acid metabolites trigger immunity
6 in *Arabidopsis* plants. *Science* **364**, 178-181 (2019). doi: [10.1126/science.aau1279](https://doi.org/10.1126/science.aau1279)

7

8 6. Y. A. Hannun, L. M. Obeid, Sphingolipids and their metabolism in physiology and
9 disease. *Nat. Rev. Mol. Cell Biol.* **19**, 175-191 (2018). doi: [10.1038/nrm.2017.107](https://doi.org/10.1038/nrm.2017.107)

10

11 7. R. Berkey, D. Bendigeri, S. Xiao, Sphingolipids and plant defense/disease: the "death"
12 connection and beyond. *Front. Plant Sci.* **3**, 68 (2012). doi: [10.3389/fpls.2012.00068](https://doi.org/10.3389/fpls.2012.00068)

13

14 8. M. S. Monjil, H. Kato, K. Matsuda, N. Suzuki, S. Tenhiro, T. Suzuki, M. Camagna, A.
15 Tanaka, R. Terauchi, I. Sato, S. Chiba, K. Kawakita, M. Ojika, D. Takemoto, Two
16 structurally different oomycete MAMPs induce distinctive plant immune responses.
17 BioRxiv (2021).

18

19 9. H. Kato, K. Onai, A. Abe, M. Shimizu, H. Takagi, C. Tateda, H. Utsushi, S.
20 Singkarabanit-Ogawa, S. Kitakura, E. Ono, C. Zipfel, Y. Takano, M. Ishiura, R.
21 Terauchi, Lumi-Map, a real-time Luciferase bioluminescence screen of mutants
22 combined with MutMap, reveal *Arabidopsis* genes involved in PAMP-triggered
23 immunity. *Mol. Plant Microbe Interact.* **33**, 1366-1380 (2020).
24 doi.org/10.1094/MPMI-05-20-0118-TA

25

26 10. Z. Zheng, S. A. Qamar, Z. Chen, T. Mengiste, *Arabidopsis* WRKY33 transcription
27 factor is required for resistance to necrotrophic fungal pathogens. *Plant J.* **48**, 592-
28 605 (2006). doi: [10.1111/j.1365-313X.2006.02901.x](https://doi.org/10.1111/j.1365-313X.2006.02901.x)

29

30 11. C. Denoux, R. Galletti, N. Mammarella, S. Gopalan, D. Werck, G. De Lorenzo, S.
31 Ferrari, F. M. Ausubel, J. Dewdney, Activation of defense response pathways
32 by OGs and Flg22 elicitors in *Arabidopsis* seedlings. *Mol. Plant.* **1**, 423-445 (2008).
33 doi: [10.1093/mp/ssn019](https://doi.org/10.1093/mp/ssn019)

1

2 12. A. Abe, S. Kosugi, K. Yoshida, S. Natsume, H. Takagi, H. Kanzaki, H. Matsumura,
3 K. Yoshida, C. Mitsuoka, M. Tamiru, H. Innan, L. Cano, S. Kamoun, R. Terauchi,
4 Genome sequencing reveals agronomically important loci in rice using MutMap. *Nat. Biotechnol.* **30**, 174-178 (2012). doi: [10.1038/nbt.2095](https://doi.org/10.1038/nbt.2095)

5

6

7 13. J. Park, T. H. Kim, Y. Takahashi, R. Schwab, K. Dressano, A. B. Stephan, P. H. O.
8 Ceciliato, E. Ramirez, V. Garin, A. Huffaker, J. I. Schroeder, Chemical genetic
9 identification of a lectin receptor kinase that transduces immune responses and
10 interferes with abscisic acid signaling. *Plant J.* **98**, 492-510 (2019). doi:
11 [10.1111/tpj.14232](https://doi.org/10.1111/tpj.14232)

12

13 14. A. Zienkiewicz, J. Gömann, S. König, C. Herrfurth, Y. T. Liu, D. Meldau, I. Feussner,
14 Disruption of Arabidopsis neutral ceramidases 1 and 2 results in specific sphingolipid
15 imbalances triggering different phytohormone-dependent plant cell death
16 programmes. *New Phytol.* **226**, 170-188 (2020). doi: [10.1111/nph.16336](https://doi.org/10.1111/nph.16336)

17

18 15. K. Umemura, S. Tanino, T. Nagatsuka, J. Koga, M. Iwata, K. Nagashima, Y.
19 Amemiya, Cerebroside elicitor confers resistance to fusarium disease in various plant
20 species. *Phytopathology* **94**, 813-818 (2004). doi: [10.1094/PHYTO.2004.94.8.813](https://doi.org/10.1094/PHYTO.2004.94.8.813)

21

22 16. P. Sperling, E. Heinz, Plant sphingolipids: structural diversity, biosynthesis, first
23 genes and functions. *Biochim. Biophys. Acta.* **1632**, 1-15 (2003). doi: [10.1016/s1388-1981\(03\)00033-7](https://doi.org/10.1016/s1388-1981(03)00033-7)

24

25

26 17. S. T. Pruett, A. Bushnev, K. Hagedorn, M. Adiga, C. A. Haynes, M. C. Sullards, D.
27 C. Liotta, A. H. Merrill Jr, Biodiversity of sphingoid bases (“sphingosines”) and
28 related amino alcohols. *J. Lipid Res.* **49**, 1621-1639 (2008). doi:
29 [10.1194/jlr.R800012-JLR200](https://doi.org/10.1194/jlr.R800012-JLR200)

30

31 18. H. Imai, Y. Morimoto, K. Tamura, Sphingoid base composition of
32 monoglycosylceramide in Brassicaceae. *J. Plant Physiol.* **157**, 453-456 (2000).
33 doi.org/10.1016/S0176-1617(00)80031-0

1

2 **Acknowledgments:** We thank H. Utsushi, E. Kanzaki, K. Ito, E. Sato (in IBRC) and Y. Inoue (in Kyoto university) for technical support. Computational analysis was partially performed on the NIG supercomputer at the ROIS National Institute of Genetics.

5 **Funding:** This work was supported by the Japan Society for the Promotion of Science KAKENHI grants (20K15528, H.K.; 15H05779 and 20H00421, R.T.; 20H02995, S.A.; 7 17H06172, K.S.; 21K19112 and 21H05032, Y.T.; 17H03963, K.K; 20H02985, D.T.).

8 **Author contributions:** H.K., D.T., Y.T., K.S., and R.T. conceived this study. H.K. performed main experiments and data analyses. M.S. and A.A. performed MutMap analysis. D.T., K.K., and M.O. purified and provided Pi-Cer D and performed HPLC analysis. K.O. and M.I. developed the bioluminescence monitoring system. S.A. and K.S. performed inoculation assays. K.N, N.I, T.D., and K.S. performed protein expression and binding assays. H.K. drafted the manuscript. H.K., D.T., Y.T. K.S., and R.T. wrote the manuscript.

15 **Competing interests:** The authors declare no conflicts of interest in relation to this work.

16 **Data and materials availability:** All data are available in the main text or supplementary 17 materials.

18 **Supplementary Materials:**

19 Materials and Methods

20 Figures S1 – S17

21 Tables S1 – S6

22 References (19 – 26)

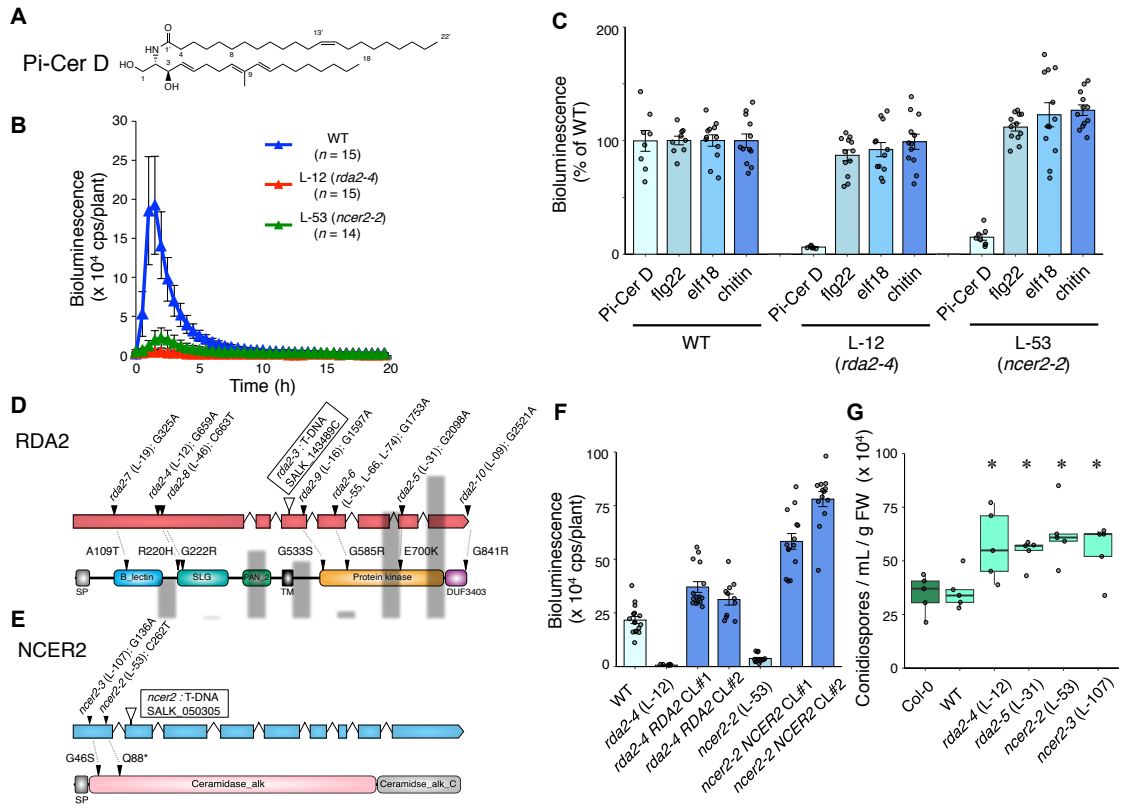
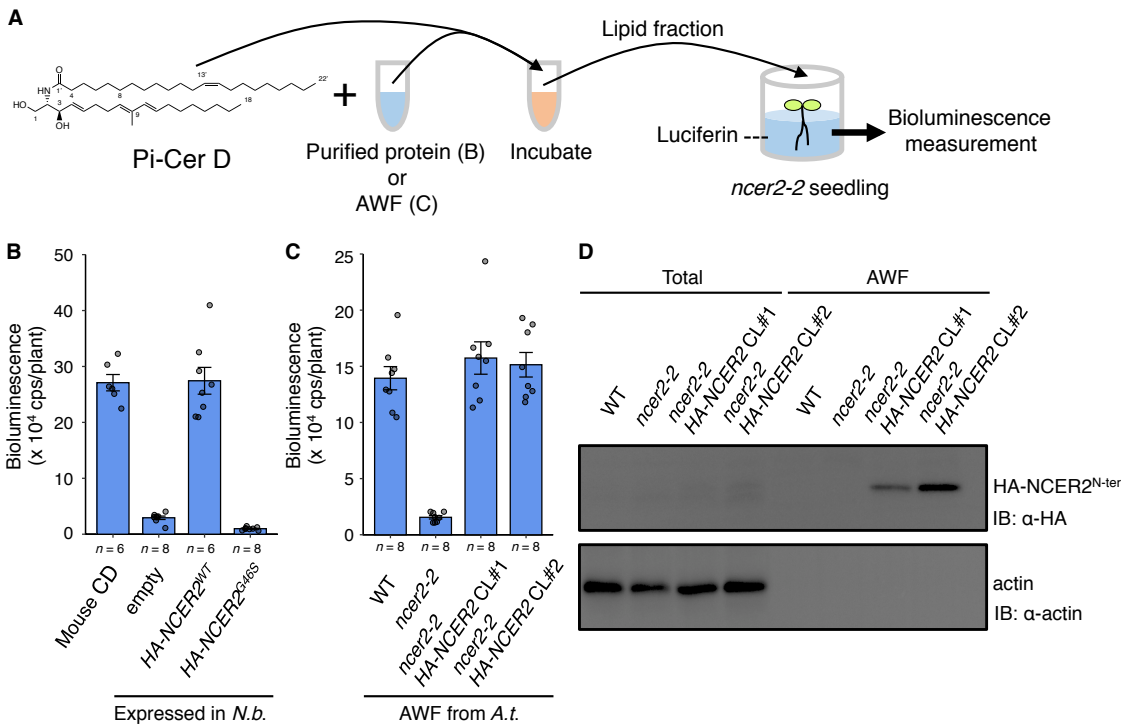
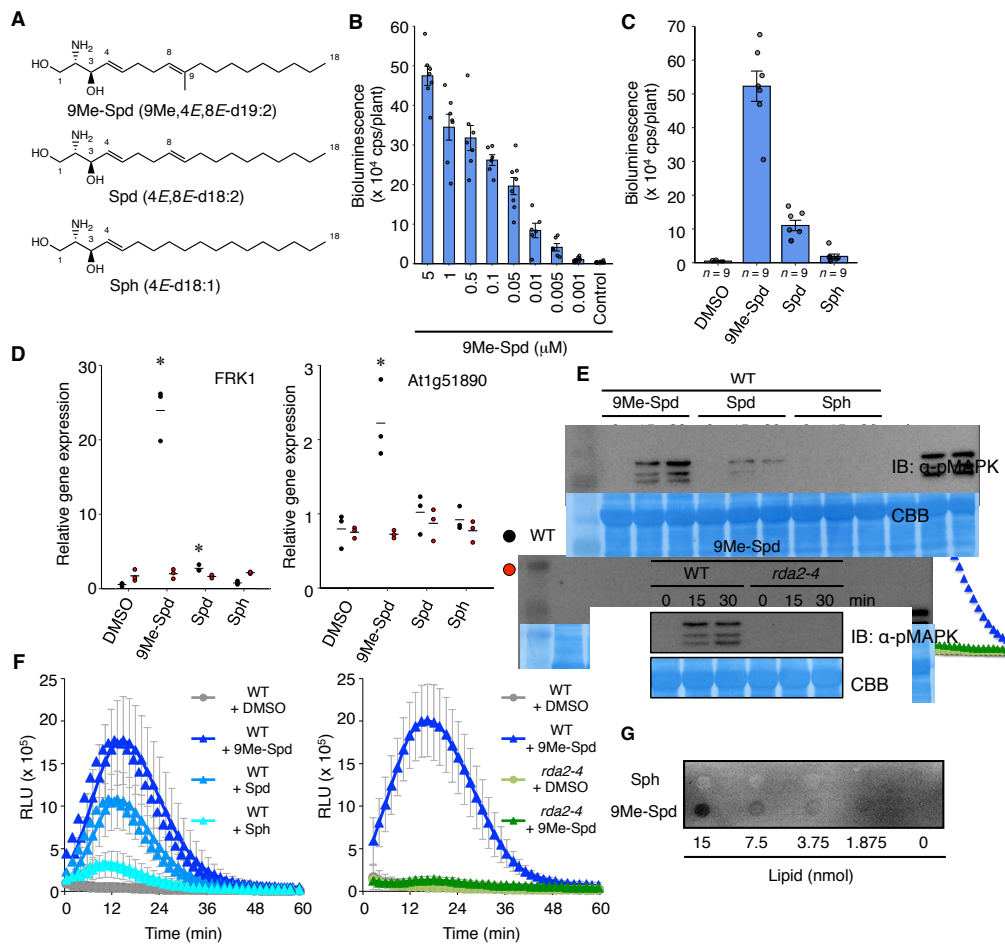


Fig. 1. Arabidopsis *RDA2* and *NCER2* are required for recognition of Pi-Cer D and resistance against *Hyaloperonospora arabidopsis* (A) Chemical structure of Pi-Cer D. (B) Bioluminescence response over time of Arabidopsis pWRKY33-LUC reporter (WT), *rda2-4*, and *ncer2-2* after Pi-Cer D (0.17 μ M) treatment (means \pm SD). For additional data, see fig. S3. (C) Bioluminescence of WT and mutant seedlings after treatment with Pi-Cer D, flg22, elf18, or chitin. Relative peak bioluminescence values are shown as % of WT (means \pm SE). For additional data, see fig. S4. (D and E) Gene and protein structures of RDA2 (D) and NCER2 (E). Gene structure (top), showing exons in boxes and introns as lines between the boxes. Protein structure (bottom), showing the different domains. The positions of the EMS-induced point mutations in different alleles (closed triangle) and T-DNA insertion sites (opened triangle) are indicated. (F) Complementation of *rda2* and *ncer2* mutants with wild-type alleles. Bioluminescence (means \pm SE) of WT, *rda2-4*, *ncer2-2*, and complemented lines (CL) after Pi-Cer D (0.17 μ M) treatment is shown. For additional data, see fig. S6. (G) Growth of *Hyaloperonospora arabidopsis* on Arabidopsis Col-0, WT, and *rda2* and *ncer2* mutants. Three-week-old Arabidopsis plants were inoculated with *Hpa* Waco9. Conidiospores were harvested and counted 5 days post inoculation ($n = 5$). *, $p < 0.05$ in two-tailed *t*-tests comparing the corresponding values from Col-0. Experiments were performed three times with similar results.



1

Fig. 2. Pi-Cer D is cleaved by NCER2, an apoplastic ceramidase. (A) Pi-Cer D-cleavage assay. Pi-Cer D was incubated for 24 h with HA-NCER2, its mutant variant produced in *Nicotiana benthamiana* leaves, or apoplast wash fluid (AWF) from *Arabidopsis* plants. The lipid fraction containing metabolites derived from Pi-Cer D was recovered and applied to *ncer2-2* plants, and their bioluminescence was measured. **(B)** Pi-Cer D is cleaved by the *Arabidopsis* ceramidase NCER2. HA-tagged wild-type (HA-NCER2^{WT}) and mutated NCER2 (HA-NCER2^{G46S}, carrying the same mutation as in the L-107 line) were transiently expressed in *N. benthamiana* (*N.b.*) and purified. Commercial mouse ceramidase (Mouse CD) served as a positive control. Peak bioluminescence is shown (means \pm SE). For additional data for NCER2 expressed in *N. benthamiana*, see fig. S8. **(C)** Pi-Cer D-cleavage activity of *Arabidopsis* (*A.t.*) AWF. AWFs were isolated from the pWRKY33-LUC reporter line (WT), *ncer2-2* and the *ncer2-2* HA-NCER2 complementation lines (CL). Peak bioluminescence is shown (means \pm SE). For additional data with *ncer2-2* HA-NCER2 plants, see fig. S9. **(D)** Immunoblot analysis of total protein and AWF extracted from WT, *ncer2-2* and *ncer2-2* HA-NCER2 plants. Anti-actin antibody was used to detect cytosolic protein. Experiments were performed three times with similar results.



1

Fig. 3. RDA2 recognizes 9-methyl sphingoid base and induces defense responses. (A) Structures of (4E,8E)-9-methyl-4,8-sphingadienine (9Me-Spd), (4E,8E)-4,8-sphingadienine (Spd), and sphingosine (Sph). **(B and C)** Peak bioluminescence values for *Arabidopsis* pWRKY33-LUC reporter seedlings (WT) treated with **(B)** different concentrations of 9Me-Spd or **(C)** 0.5 μ M of structurally different sphingoid bases (means \pm SE). For additional data, see fig. S12 and S13. **(D)** Expression of defense genes (*FRK1* and *At1g51890*) in *Arabidopsis* seedlings 3 h after elicitation with sphingoid bases (0.5 μ M) relative to expression in DMSO-treated WT. Individual data (symbols) and means (bars) are shown ($n = 3$); *, $p < 0.05$ (two-tailed *t*-test). **(E)** Mitogen-activated protein kinase (MAPK) activation following treatment with sphingoid base (0.5 μ M). Phosphorylated MAPKs were visualized with anti-phospho-p44/p42 MAPK antibody. **(F)** ROS accumulation in *Arabidopsis* leaves treated with sphingoid bases. Left, leaf disks from WT plants treated with 30 μ M 9Me-Spd, Spd, or Sph ($n = 12$). Right, leaf disks from WT and *rda2-4* plants treated with 30 μ M 9Me-Spd ($n = 10$). Relative light unit (RLU) is shown (means \pm SD). **(G)** Binding of sphingoid bases with HA-tagged RDA2 by protein-lipid overlay assay. For additional data, see fig. S16 and S17. Experiments were performed two **(B, D, and F)** or three times **(C, E, and G)** with similar results.

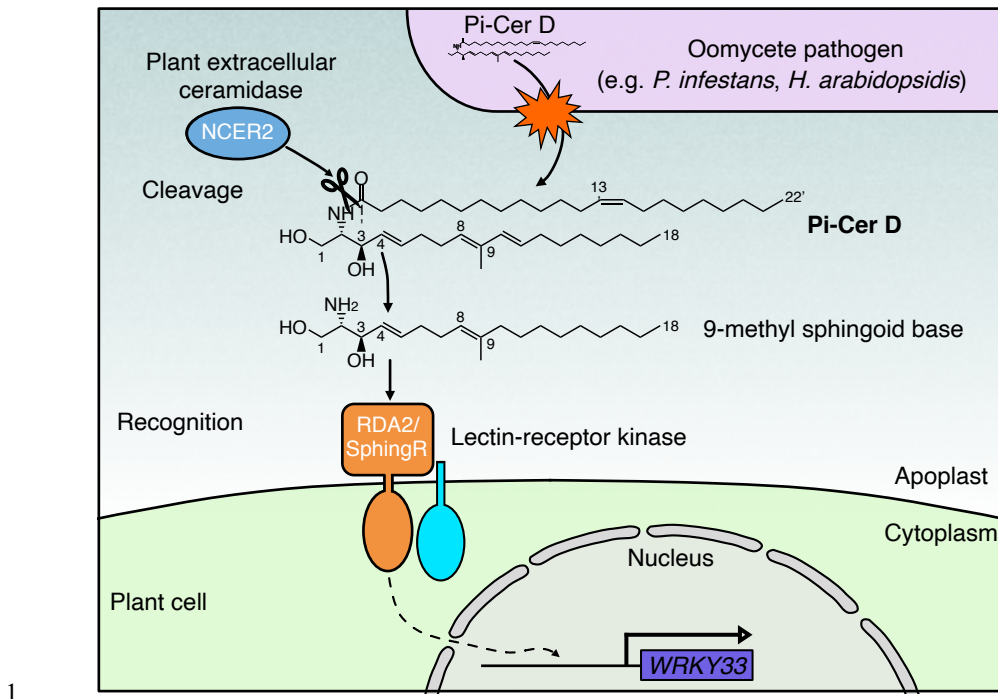


Fig. 4. A model for the recognition of pathogen-derived ceramide in plants. Pi-Cer D is cleaved by plant apoplastic ceramidase NCER2 into 9-methyl sphingoid base. 9-methyl sphingoid base is recognized by a lectin-receptor kinase, RDA2/SphingR, which then induces defense responses that include *WRKY33* gene expression and enhances immunity against pathogen infection.